AIChE Journal
DOI 10.1002/aic.15631

Synthesis and optimization of membrane cascade for gas separation via mixed-integer nonlinear programming (MINLP)

Alicia Aliaga-Vicente, José A. Caballero, María J. Fernández-Torres*

Department of Chemical Engineering, University of Alicante., Ap. Correos 99, 03080, Alicante, Spain.

**corresponding author: fernandez@ua.es*

ABSTRACT

Currently, membrane gas separation systems enjoy widespread acceptance in industry As multistage systems are needed to achieve high recovery and high product purity simultaneously, many such configurations are possible. These designs rely on the process engineer's experience and therefore sub-optimal configurations are often the result. This paper proposes a systematic methodology for obtaining the optimal multistage membrane flowsheet and corresponding operating conditions. The new approach is applied to cross-flow membrane modules that separate CO_2 from CH_4, for which the optimization of the proposed superstructure has been achieved via a MINLP model, with the gas processing cost as objective function. The novelty of this work resides in the large number of possible interconnections between each membrane module, the energy recovery from the high pressure outlet stream and allowing for non-isothermal conditions. The results presented in this work comprise the optimal flowsheet and operating conditions of two case studies.

This article has been accepted for publication and undergone full peer review but has not been through the copyediting, typesetting, pagination and proofreading process which may lead to differences between this version and the Version of Record. Please cite this article as doi: 10.1002/aic.15631

Received: Jun 15, 2016; Revised: Dec 16, 2016; Accepted: Dec 27, 2016

KEYWORDS

Gas separation; Membrane cascade; Process synthesis; Disjunctive model; MINLP

Introduction

Membrane gas separation processes have grown in importance within the chemical industry in the last three decades, particularly since the early 1980s when polymeric membranes started to become economically feasible[1,2]. However, the large-scale industrial applications of this technology are still far from reaching the true potential that this separation unit operation offers[2].

Nowadays, around 90-95% of separations and purifications are performed by distillation, a fact that is likely to change in the near future[3,4]. The current membrane market share is about 2%, but this fraction is expected to increase[5]. In the case of gas separation, membrane systems compete with conventional technologies such as cryogenic distillation or pressure swing adsorption. This is because membrane gas separation has become a viable alternative and offers additional advantages including, but not limited to, simplicity of operation, compactness, a small environmental footprint and mechanical reliability. These attributes make it a very interesting separation technology for offshore installations[1,2,6,7]. Some of the main industrial applications developed for membrane gas separation are[2]: removal of nitrogen from air; enrichment of oxygen from air; separation of hydrogen from gases like nitrogen and methane; removal of acidic gases (CO_2 and/or H_2S) from crude natural gas; air and natural gas dehydration; and separation and recovery of volatile organic liquids from air in exhaust streams. For these applications, a multistage system involving recycle-compressors is usually needed to simultaneously achieve higher purities and recoveries at lower energy consumption and large capacities.

The most common membrane cascade scheme[8] is shown in Figure 1.a. In the notation and numbering appearing in this figure, the unit next to the feed stream is assigned the number 1; E stands for a membrane unit in the enriching section and S for a membrane in the stripping section; CE and CS stand for compressor in the enriching and stripping sections, respectively. When the feed stream enters the membrane module, a portion of it passes through the membrane from the high to the low pressure side. This new stream is called the "permeate", while the remaining feed (not passing through the membrane), is called the "retentate". The schematic representation of the multiple membrane stages in Figure 1.a shows that part of the permeate from one stage (a lateral permeate extraction) is first compressed and, then, sent as feed to the previous stage; while the retentate stream from each stage is mixed with the above mentioned compressed stream and sent to the succeeding stage.

In order to design and develop an economically viable membrane separation system, a process engineer has traditionally had to focus on selecting an appropriate configuration and determining the optimal operating conditions of each membrane and compressor[7]. The first aspect is critical due to the fact that there is a trade-off between the power consumption and the capital cost; energy requirements normally diminish as the number of recycle streams increases, but then the capital cost related with recycle-compressors tends to grow. Most of the existing literature on this matter mentions the fact that this trade-off is generally solved by choosing cascades with fewer compressors[9].

Currently, the development of membrane cascade schemes involves using a sequential procedure in which a particular flow diagram of a membrane system is first selected by the process engineer and then, after that, the operating conditions are optimized. However, few alternative flowsheets are typically considered and this approach is traditionally carried out by experienced design engineers as was pointed out by Qi and Henson[7].

In the last decades, various researchers have analysed a small number of simple membrane configurations. Agarwal and Xu[10,11] and Agrawal[12] developed a stepwise procedure for obtaining membrane cascades with a limited number of recycle compressors. Qi and Henson[7] investigated the economic feasibility of multistage membrane systems for multicomponent gas mixtures. Kookos[1] studied membrane systems and membrane material impact.

The aim of the present research is to develop a systematic methodology for obtaining the optimal flowsheet and corresponding operating conditions of a multistage membrane system at minimum gas processing cost. Although such an approach has been employed previously[1,7,13,14], the cited studies have not considered a number of important aspects. In this paper, some of these novel aspects, such as, a turbine at the exit product retentate stream, possible lateral extraction streams, and temperature changes during the compression have also been considered. To that end, we propose to formulate the present design problem as a mixed-integer nonlinear programming

(MINLP) problem, which allows simultaneous optimization of the membrane configuration and the corresponding operating conditions.

Case studies

Two case studies of the separation of CO_2 from CH_4 have been selected to demonstrate how well the proposed MINLP works: crude natural gas sweetening and enhanced oil recovery (CO_2 enrichment)[15-17]. The binary mixture under study has been selected, in particular, due to the fact that the total worldwide production of natural gas is about 1.13×10^{12} standard cubic meters/year. Of this gas approximately 20% requires extensive treatment before it can be delivered to the pipeline. No other mixture has been considered because this example is also of great social, economic and environmental importance to the capture and sequestration of CO_2. In the present work, the optimal design strategy is applied to hollow fibre membrane modules (made of polyimide), operating in cross-flow mode to separate the above binary mixture. Polyimide membranes have been chosen because of their high permeability to CO_2 and good selectivity against CH_4. This material is usually shaped into hollow fibre modules, which can achieve higher area per unit volume than spiral wound modules[18].

Problem statement

In this work, the problem of synthesizing membrane cascades for binary gas separations can be expressed as follows: Given the feed characteristics and a superstructure which embeds the most meaningful process flowsheet alternatives, determine the optimal process layout and operating conditions (pressures, areas, flow rates…) that simultaneously minimize an economic indicator (the gas processing cost) and accomplish the binary separation. The economic parameters as well as the membrane properties are assumed to be known.

In order to solve the problem, the superstructure is formulated as a MINLP model, accompanied by the following assumptions:

- Ideal gas behaviour.
- Steady-state conditions.
- Constant permeabilities (independent of temperature, pressure and gas composition).
- Known characteristics of the feed stream and product permeate pressure.
- The retentate experiences no pressure drop between membrane stages.
- Negligible axial diffusion and concentration polarization effects.
- Negligible deformation of the fibres under pressure.

Methodology

The first step in the optimization procedure involves postulating a superstructure that embeds many process configurations, each representing a candidate optimal process flowsheet. After that, the superstructure is mathematically described via a model (containing both continuous and integer variables, encompassing operating conditions, the inclusion or not of process units and their corresponding interconnections). To solve this MINLP problem, we employ the SBB algorithm (which is based on a combination of the Standard Branch and Bound method and other NLP solver: CONOPT), within the General Algebraic Modelling System (GAMS)[19].

Before introducing the superstructures used in this research, we need to describe how to characterize membrane cascades.

Characterization of membrane cascades. In the present research, the postulated superstructures are based on the work by Agrawal and Xu work[9]. According to them, in general, a membrane cascade scheme is defined by two parameters: p and q.

- The parameter p represents the number of previous membrane stages that the compressed permeate is fed to.
- The parameter q refers to the number of succeeding membrane stages that the retentate is sent to.

For example, the configuration shown in Figure 1.a is a symmetrical cascade in which the value of both parameters is 1 (p = 1, q = 1).

If the value of p is 2 (p = 2, q = 1), the cascade is unsymmetrical and the compressed permeate of one stage becomes part of the feed of the membrane stage immediately before the previous one. As q = 1, the retentate is sent to the succeeding stage. This scheme is illustrated in Figure 1.b.

Conversely, if the value of q is 2 (p = 1, q = 2), the cascade is unsymmetrical as well, but the retentate of one stage is sent as feed to the membrane stage immediately after the next one. As p = 1, the compressed permeate is fed to the previous stage. For clarity, this configuration is illustrated in Figure 1.c.

It is worth noting that the symmetrical cascade shown in Figure 1.a is embedded in both unsymmetrical cascades (Figures 1.b and 1.c), based on the observation that if membrane stages (E2, S1, S3) are removed from any of the unsymmetrical cascades (p = 2, q = 1 or p = 1, q = 2), the resulting structure is equivalent to the symmetrical cascade. For this reason, both unsymmetrical schemes are more general and contain more feasible substructures. Consequently, they are referred to as "parent cascades".

Although the unsymmetrical cascades correspond to a value of p (or q) of 2, it is possible to draw more schemes for other values. However, if the values of p and q of a cascade have a common factor (different from one), the structure is equivalent to independent parallel cascades with the minimum common factor of p and q. For example, a cascade with p = 2 and q = 4 corresponds to two independent parallel cascades with p = 1 and q = 2.

Membrane cascade superstructures. It is first necessary to propose a superstructure that embeds many potentially advantageous configurations if the optimization problem is to be tackled effectively. The design of this superstructure is a crucial step, because a possible solution will not be generated if it is not contained within the superstructure. The superstructures that will be used here have been constructed from the parent cascades introduced above. However, we include additional elements, which represent part of the novelty that can be attributed to this work:

(i) A turbine at the exit product retentate stream (at high pressure). We consider the possibility of work integration between compressors and turbines by means of a common shaft. We are assuming, therefore, that the aim is not to stock the exiting gas under high pressure;

(ii) We allow for the membrane system to be non-isothermal, the result of temperature changes during membrane separations and permeate compressions. Because of these temperature changes, we have introduced heat exchangers in the compressor outlet streams, in order to decrease their temperature before they come into contact with the membrane (membranes are damaged by high temperatures). Such temperature changes have been investigated by Gorissen[20] and Ahmad et al.[21], but their results have not been applied to the optimization of the process layout. The investment in coolers (and cooling utilities) and the effect of temperature on compressor performance (performance improves at lower inlet gas temperatures) could eventually have an important impact on the economics of the process.

(iii) We use a novel staged-based superstructure. The superstructure is based on previous work done by Agrawal et al[8-12]. They established the theoretical basis for membrane cascades and presented detailed sensitivity studies of different parameters, but did not perform economic optimization. Another alternative would be to use a superstructure whose various membranes are fully interconnected. However, such superstructures tend to lead to very complex problems from a mathematical point of view (highly non-convex and with many bilinear terms), and usually cannot be solved for a global optimum. They also tend to deliver complex results that in many cases entail difficult controllability and are limited to a small number of stages. This idea is not new; for instance, the superstructure that probably enjoys the most success in the design of heat exchangers was proposed by Yee and Grossmann[22]. It is stage-based and sacrifices some of the possible final configurations if they are found to be present in other complex superstructures. The superstructure considered contains possible lateral extraction streams. It also has been augmented with bypasses and other streams in order to expand the space of alternatives based on physical reasoning, instead of using a 'full connectivity approach'. In this way we can postulate alternatives encompassing a relatively large number of membrane modules with a very low probability of 'losing the optimal solution'.

In this paper two different superstructures consisting of fourteen stages each, are postulated:

- Unsymmetrical cascade with p = 2, q = 1 (Figure 2).
- Unsymmetrical cascade with p = 1, q = 2 (Figure 3).

A number of details in Figure 2 require further explanation: first, the low pressure feed is compressed in the compressor C_{feed} and subsequently fed directly to the high pressure side of the membrane unit S1. There are two possibilities for the retentate stream from each stage in Figure 2 (which can be identified quite easily by looking at two consecutive stages, e.g, S1 and S2): the retentate stream can either feed the succeeding membrane unit (S2), or bypass it and all the consecutive membrane units in the stripping section via a lateral extraction that must, by construction, end up in the turbine after membrane unit S7 (to take advantage of its high pressure). Our optimization procedure allows for the simultaneous existence of these two options. The retentante stream from each stage in Figure 3 implies a third additional option: it can feed the stage after the succeeding one (e.g. run directly from S1 to S3). These three options are also simultaneous possibilities. Turning our attention now to the permeate stream in Figure 2, it too is associated with three options: (1) it can be sent as sweep stream to the previous membrane (no intervening compression, e.g., the permeate of S4 passes directly to the permeate side of S3); (2) it can be compressed and sent to the stage before the previous one (e.g., the permeate from S4 is compressed in CS2 and then combined with the feed stream to S2); or, (3) it can simply exit the system by lateral extraction. These three options can exist simultaneously. Finally, the three options described above likewise apply to the permeate streams in Figure 3, except for the permeate stream of, for instance, S4: once it has been compressed, it will be added to the feed stream to membrane unit S3, instead of membrane unit S2. Unsurprisingly, these three options are also a simultaneous possibility. In both Figures 2 and 3, the outlet retentate stream, which includes the retentate of the last stage and all of the lateral retentate extractions, is sent to a turbine. Because this stream is at a high pressure, some electricity can be saved by operating the turbine and recycle compressors along a common shaft. It is worth noting that each membrane stage can operate at different pressure ratios. As pointed out earlier regarding Figures 1.b and 1.c, under the heading “characterization of membrane cascades”, Figures 2 and 3 can also be converted to symmetrical cascades by removing a number of membrane modules.

Optimization model formulation

In this section we present the mathematical formulation of the optimization procedure, the details of the economic evaluation that has been performed, and the data used in the optimization calculi. At the end, we include a list of the aspects of our formulation that make it novel.

Mathematical formulation. The superstructures of both membrane cascades shown in Figures 2 and 3 are mathematically formulated as a Generalized Disjunctive Programming (GDP) problem, shown in Figure 4 (two mathematical models), where x is a vector of continuous variables which represent pressures, flow rates and membrane areas of the process. The objective function z represents the gas processing cost (GPC) which will be discussed in the next section. The set of equality constraints $h(x) = 0$ correspond to material balances and equipment equations; whereas the set of inequalities $g(x) \leq 0$ denote design specifications. Each term of the disjunction k represents the possible existence of the equipment unit i, and is associated with a Boolean variable Y_{ik} and a set of constraints $r_{ik}(x) \leq 0$ and $s_{ik}(x) = 0$ (costs, material balances, etc). When the term is active ($Y_{ik} = True$), the corresponding constraints have to be satisfied; whereas they will be ignored if the term is not active. Finally, the equations $\Omega(Y) = True$ represent logic propositions relating the disjunctions.

The detailed mathematical formulation of the unsymmetrical cascade superstructures, shown in Figures 2 and 3, appears in Appendices A and B, respectively. Both models, separately, serve to optimize the two case studies. The reason for this is that it would be difficult to merge both superstructures (and mathematical models) into one.

Economic assessment. In these case studies, the cost of removing CO_2 from natural gas to accomplish the pipeline specifications (here denoted as Gas Processing Cost, GPC) is defined as the cost to treat 26.84 standard m^3 measured at 101.325 kPa and 0ºC. This calculation is based on the economic analysis presented by Hao et al.[14] , but also includes cooling costs of multi-stage compressors and various investment cost correlations for compressors, heat exchangers and turbines. Table 1 contains a detailed description of the calculation process that has been followed. The value of the GPC takes into account the Capital Related Cost (CRC), the Variable Operating and Maintenance cost (VOM) and the cost of CH_4 losses in the permeate (CH_4LS). The project contingency, which includes all unpredictable elements of the project, is assumed to be 20% of the base plant cost. In order to calculate the capital cost, a payout time of 5 years has been assumed. This assumption is necessary because the costs, and not the profits, are calculated. The payout time is fixed *a priori* and, afterwards, the total annualized cost is computed by taking into account this basis of calculation. It is worth noting that Table 1 also includes a number of other assumptions about the performed calculations, such as the value of the membrane lifetime that has been considered (4 years).

According to the literature[5], the cost of a hollow fibre module, including the membrane elements, is about \$50/m^2. Moreover, the replacement cost of the membrane element is \$25/m^2. A related consideration concerns the wellhead price of natural gas, because it depends on the market and can rise or fall rapidly. In this study, the wellhead price of natural gas is assumed to be 1.9 \$/GJ [13,14].

Data used in the optimization calculi

For the sake of simplicity, the feed is regarded as a binary mixture instead of wellhead natural gas, which is multi-component and complex. Furthermore, the hollow-fibre membrane modules, of a shell-side feed design (the permeate passes through the fibre wall and exits through the open fibre ends), operate in cross-flow mode. The parameters and conditions that optimize each case study are presented in Tables 2 and 3. Table 2 shows the assumed membrane properties while Table 3 lists the data that has been collected on the two case studies. A typical value of 0.5×10^{-6} m for the effective membrane thickness is assumed. It is worth pointing out from Table 3 that the recovery of CH_4 must be greater than 95% and that, in addition, the retentate mole fraction of CO_2 must be smaller than or equal to 0.02 in both case studies. This table also shows that the permeability is assumed to be a constant value, independent of temperature, since it is usually accepted that permeation through the membrane is an isenthalpic process, which implies a small temperature change that has been corroborated according to the results obtained. This assumption is also made by Binns et al[25] in their study of the best strategies to simulate multi-component and multi-stage membrane gas separation systems; and by Gilassi and Rahmanian[26], in the mathematical modelling and simulation of CO_2/CH_4 separation by means of a polymeric membrane. It is only recently that a pressure-variable value of the permeability has been considered in the simulation of a membrane gas separation[27].

Results

Before discussing the results, it is worthwhile to remind the reader that the case studies are optimized by applying both mathematical models described in appendices

A and B (or both superstructures shown in Figures 2 and 3). The optimized result presented here derives from the model that, of the two, produces the lowest cost. A summary of the model statistics and CPU time required for each case study is shown in Table 4.

Optimized flowchart diagram for the crude natural gas sweetening. It is essential to treat the natural gas such that it meets pipeline specifications (CO_2 composition lower or equal than 2% vol.) because CO_2 is corrosive and reduces the heating value and dew point of natural gas.

Figure 5 shows the optimal flowsheet and operating conditions for the crude natural gas sweetening process, obtained in this work. The molar fraction of the feed stream is 0.9 CH_4 and 0.1 CO_2, as shown in Table 3. The optimal process layout has been obtained from the parent membrane cascade p = 2, q = 1 (the superstructure in Figure 2). As was expected, due to the high compressor costs, there are few compressors (this flowsheet has only two compressors). Both specifications (recovery and retentate purity) are satisfied and the gas processing cost is 0.00969 \$/($m^3_{(STP)}$/day). Figure 5 also shows the layout of the remaining elements in the original superstructure in a way that is easy to recognise, but the underlying intention of the calculation is to arrange the three compressors and turbine along the same shaft. This is done to emphasize that it is possible to recover, via the turbine, part of the energy spent in the pressurized streams. This arrangement (same shaft) is shown explicitly in Figure 6.

Enhanced oil recovery (CO_2 enrichment). Enhanced oil recovery is a technique based on the injection of oil-miscible gases (such as CO_2) to increase the amount of oil or gas extracted from a petroleum reservoir. Membrane separation is useful to recover, for the purposes of reuse, the CO_2 injected into the natural gas. It is set up in such a way that the CO_2 concentration in the permeate stream has to be higher than 95 % vol[30]. The optimal flowsheet and process details for this case study are shown in Figure 7 and satisfies all the specifications (recovery and purities). As in the other case study, there are few compressors (just one in this case). The gas processing cost for this case study is 0.01738 \$/($m^3_{(STP)}$/day).

Sensitivity analysis. In order to assess the sensitivity of these results, different molar fractions of the feed stream have been tested in the first case study, i.e., crude gas sweetening: from 0.2 to 0.95 for species CH_4, but holding the total molar flow rate in the feed stream constant. This sensitivity analysis must also obey the constraints shown in Table 3, namely, recovery of CH_4 above 95% and a maximum retentate mole fraction of 2% for CO_2. Figure 8 shows the objective function (GPC) as a function of the feed composition. Obviously, the richer in CH_4 the stream, the cheaper is the purification process. Also, it is interesting to observe how the optimized layout changes with feed composition while the total molar flow rate in the feed stream is held constant. This is shown in Figure 9 where, in order to satisfy the condition that there be at most 2% CO_2 in the retentate stream, the system must experience an increase in the mole percentage of CO_2 in the permeate stream (and a simultaneous increase in the recovery of CH_4, up to 99.92%). This becomes possible only when the complexity of the layout is also increased. Therefore, there is a feed mole fraction value (around 60% CH_4) for which the total number of stages decrease to a minimum (one stage). By lowering the concentration of CH_4, the optimized layout becomes more expensive as shown in Figure 8. This is due to the pressure value and the recovery of energy in the turbine.

Conclusions

A systematic methodology for obtaining the optimal flowsheet and corresponding operating conditions for a multistage membrane system at minimum gas processing cost has been developed in this paper. Two case studies have been treated by means of a MINLP model that allows simultaneous optimization of the membrane cascade configuration and the operating conditions. To illustrate this procedure, the separation of CO_2 from CH_4 with hollow fibre membranes has been carried out under two different scenarios: a) crude natural gas sweetening and b) enhanced oil recovery. Moreover, a sensitivity analysis has been performed from which it can be concluded that our model is able to select the optimized layout for a change in any desired parameter, e.g., the feed composition. This analysis proves that a feed mole fraction of around 60% CH_4 minimizes the number of membrane stages, and that this number (of stages) and the complexity of the layout increases upon increasing or decreasing the mole fraction in question.

Our results highlight the benefit of using a rigorous optimization approach: it has allowed us to obtain the optimal operating conditions *and* optimal process layout by means of the MINLP model proposed here.

Finally, it is not possible to guarantee a globally optimal solution since the problem is non-linear and non-convex.

Acknowledgments

We thank Mr. W. Dednam for proofreading this article. The authors also thank the other members of our research group (COnCEPT – Computer OptimizatioN of Chemical Engineering Processes and Technologies) for constructive discussions (http://web.ua.es/en/concept/concept-computer-optimization-of-chemical-engineering-processes-and-technologies.html).

Notation

Sets

$$COMP := \{ j \mid j \text{ is a compound} \}$$

$$MEM := \{ m \mid m \text{ is a membrane module} \}$$

Variables

$Area_{HE,FC}$	Area of feed heat exchanger (m^2)
$Area_{HE}{}^{m}$	Area of heat exchanger m (m^2)
$(Area_M)^m$	Area of hollow fibre membrane m (m^2)
BPC	Base plant cost ($)
$C_{Cooling}$	Annual cooling cost ($ y^{-1})
$C_{Electricity}$	Annual electricity cost ($ y^{-1})
$C_p{}^m$	Heat capacity of CP^m feeding membrane m (kJ /(kmol K))
$C_{p,feed}$	Heat capacity (kJ $kmol^{-1}$ K^{-1})
CC	Installed compressor cost ($)
$CC_C{}^m$	Installed cost of recycle-compressor m ($)
CC_{FC}	Installed feed compressor cost ($)
CHE	Installed heat exchanger cost ($)
$CHE_C{}^m$	Installed cost of heat exchanger m ($)
CHE_{FC}	Installed feed heat exchanger cost ($)
CH_4LS	Annual cost of CH_4 lost in permeate ($ y^{-1})
CMC	Annual contract and material maintenance cost ($ y^{-1})

CP^m, CP_j^m	Total and individual compressed permeate mole flow of component *j* feeding the membrane *m* (kmol s^{-1})
CRC	Annual capital related cost (\$ y^{-1})
CT	Installed turbine cost (\$)
DL	Annual direct labor cost (\$ y^{-1})
EP	Electricity price (\$ kWh^{-1})
F^m, F_j^m	Total and individual mole flow of component *j* entering the membrane m (kmol s^{-1})
FC	Fixed cost (\$)
$Feed, Feed_j$	Total and individual mole flow of feed entering the membrane cascade (kmol s^{-1})
JA^m, JA_j^m	Total and individual mole flow of component *j* across membrane *m* (kmol s^{-1})
$(LE_P)^m, (LE_P)_j^m$	Total and individual mole flow of component *j* of lateral permeate extraction from membrane *m* (kmol s^{-1})
$(LE_R)^m, (LE_R)_j^m$	Total and individual mole flow of component *j* of lateral retentate extraction from membrane *m* (kmol s^{-1})
LOC	Annual labor overhead cost (\$ y^{-1})
LTI	Annual local tax and insurance cost (\$ y^{-1})
MC	Total membrane module cost (\$)
ML	Membrane life (y)

MRC	Annual membrane replacement cost (\$ y^{-1})
N^m	Number of stages in compressor m
N_{FC}	Number of stages in feed compressor
$N^\circ workers$	Number of workers
OSF	On-stream factor
P^m, P_j^m	Total and individual permeate mole flow of component *j* of membrane *m* (kmol s^{-1})
p_{feed}	Feed pressure (Pa)
p_{in}	Membrane inlet pressure (Pa)
p_{limit}	Maximum pressure allowed (Pa)
p_{out}^m	Outlet pressure of membrane m (Pa)
$p_{out,T}$	Turbine outlet pressure (Pa)
PC	Project contingency (\$)
$(Perm)$	Permeability of membrane (kmol s^{-1} m^{-2} Pa^{-1})
$Permeate_j$	Total permeate flow rate of component *j* (kmol s^{-1})
$Q_C{}^m$	Heat exchanged between CP^m & cooling water (kW)
Q_{FC}	Heat exchanged between feed & cooling water (kW)

R^m, R_j^m	Total and individual retentate mole flow of component *j* of membrane *m* (kmol s^{-1})
R_p	Universal gas constant (kJ kmol^{-1} K^{-1})
$Recovery$	Recovery of CH_4 (%)
$Retentate_j$	Total retentate flow rate of component j (kmol s^{-1})
RP	Refrigeration price (\$ MJ^{-1})
rp^m	Compression ratio of compressor m
rp_{FC}	Compression ratio of feed compressor
RR^m, RR_j^m	Total and individual retentate mole flow of component *j* of membrane *m*, downstream lateral retentate extraction (kmol/s)
$RR1^m, RR1_j^m$	Total and individual retentate mole flow of component *j* of membrane *m*, downstream lateral retentate extraction (kmol s^{-1}). It feeds the succeeding stage.
$RR2^m, RR2_j^m$	Total and individual retentate mole flow of component *j* of membrane *m*, downstream lateral retentate extraction (kmol s^{-1}). It feeds the stage after the succeeding one.
S^m, S_j^m	Total and individual sweep mole flow of component *j* entering the membrane *m* (kmol s^{-1})
SC	Start-up cost (\$)
SCE	Stage cut (ratio between Permeate and Feed) (%)
$(sr_{CP})^m$	Split ratio of P_j^{m+1} to obtain CP_j^m

$\left(sr_{LE_P}\right)^m$	Split ratio of P_j^m to obtain LE_j^m
$\left(sr_{RR}\right)^m$	Split ratio of R_j^m to obtain RR_j^m
$\left(sr_{RR1}\right)^m$	Split ratio of R_j^m to obtain $RR1_j^m$
$\left(sr_{RR2}\right)^m$	Split ratio of R_j^m to obtain $RR2_j^m$
T_{feed}	Feed temperature (ºC)
T_{in}	Membrane inlet temperature (ºC)
$T_{in,CW}$	Inlet temperature of cooling water (ºC)
T_{limit}	Maximum temperature allowed by membranes (ºC)
$T_{out,C}{}^m$	Outlet temperature of compressor m (ºC)
$T_{out,CW}$	Outlet temperature of cooling water (ºC)
$T_{out,FC}$	Outlet temperature of feed compressor (ºC)
$\left(T_{out,M}\right)_j$	Outlet temperature of membrane m of component *j* (ºC)
$\left(T_{out,M}\right)^m$	Outlet temperature of membrane m (ºC)
TFI	Total facilities investment ($)
TPI	Total plant investment ($)

U	Overall heat exchanger coefficient (W m^{-2} K^{-1})
UC	Annual utility cost (\$ y^{-1})
VOM	Annual variable operating and maintenance cost (\$ y^{-1})
$W_C{}^m$	Work of compressor feeding membrane m (kW)
W_{FC}	Work of feed compressor (kW)
W_T	Turbine work (MW)
x_j^m	Molar fraction of component j in retentate stream of membrane m
x_{out,CO_2}	Retentate purity of CO_2
$y_C{}^m$	Choice of compressor m (if = 1)
y_j^m	Molar fraction of component j in permeate stream of membrane m
$y_M{}^m$	Choice of membrane m (if = 1)
y_{out,CO_2}	Permeate purity of CO_2
y_T	Choice of turbine (if = 1)
z_j^{Feed}	Molar fraction of component j in crude natural gas feed
z_j^m	Molar fraction of component j in feed stream of membrane m

Greek symbols

α	Membrane selectivity
γ	Ratio Cp/Cv
ΔT_{min}	Minimum approach temperature (ºC)
$\Delta T_{ML,FC}$	Logarithmic mean temperature difference in feed heat exchanger
$\Delta T_{ML}{}^{m}$	Logarithmic mean temperature difference in heat exchanger m
η	Isentropic efficiency
$\theta_{1,FC}$	Temperature difference 1 in feed heat exchanger (ºC)
$\theta_1{}^{m}$	Temperature difference 1 in heat exchanger *m* (ºC)
$\theta_{2,FC}$	Temperature difference 2 in feed heat exchanger (ºC)
$\theta_2{}^{m}$	Temperature difference 2 in heat exchanger *m* (ºC)

Literature Cited

1. Kookos IK. A targeting approach to the synthesis of membrane networks for gas separations. *Journal of Membrane Science.* 2002;208(1–2):193-202.
2. Bernardo P, Drioli E, Golemme G. Membrane Gas Separation: A Review/State of the Art. *Ind. Eng. Chem. Res.* 2009/05/20 2009;48(10):4638-4663.
3. Soave G, Feliu JA. Saving energy in distillation towers by feed splitting. *Appl. Therm. Eng.* 2002;22(8):889-896.
4. Caballero JA, Grossmann IE. *Optimization of Distillation Processes. In: A. Górak & E. Sorensen (Eds.), Distillation Fundamentals and Principles. London*: Elsevier.; 2014: 347-500.
5. Baker RW. *Membrane technology and applications*. 2nd ed. Chichester ; New York: J. Wiley; 2004.
6. Tessendorf S, Gani R, Michelsen ML. Modeling, simulation and optimization of membrane-based gas separation systems. *Chem. Eng. Sci.* 1999/04/01 1999;54(7):943-955.
7. Qi R, Henson MA. Membrane system design for multicomponent gas mixtures via mixed-integer nonlinear programming. *Comput. Chem. Eng.* 2000;24(12):2719-2737.
8. Pathare R, Agrawal R. Design of membrane cascades for gas separation. *Journal of Membrane Science.* 2010;364(1–2):263-277.
9. Agrawal R, Xu J. Gas-separation membrane cascades utilizing limited numbers of compressors. *AIChE J.* 1996;42(8):2141-2154.
10. Xu J, Agrawal R. Gas separation membrane cascades I. One-compressor cascades with minimal exergy losses due to mixing. *Journal of Membrane Science.* 1996/04/17 1996;112(2):115-128.
11. Agrawal R, Xu J. Gas separation membrane cascades II. Two-compressor cascades. *Journal of Membrane Science.* 1996/04/17 1996;112(2):129-146.
12. Agrawal R. A simplified method for the synthesis of gas separation membrane cascades with limited numbers of compressors. *Chem. Eng. Sci.* 1997/03/01 1997;52(6):1029-1044.
13. Ahmad F, Lau KK, Shariff AM, Murshid G. Process simulation and optimal design of membrane separation system for CO2 capture from natural gas. *Comput. Chem. Eng.* 2012;36:119-128.
14. Hao J, Rice PA, Stern SA. Upgrading low-quality natural gas with H2S- and CO2-selective polymer membranes: Part II. Process design, economics, and sensitivity study of membrane stages with recycle streams. *Journal of Membrane Science.* 2008;320(1–2):108-122.
15. Adewole JK, Ahmad AL, Ismail S, Leo CP. Current challenges in membrane separation of CO2 from natural gas: A review. *International Journal of Greenhouse Gas Control.* 2013;17:46-65.
16. Zhang Y, Sunarso J, Liu S, Wang R. Current status and development of membranes for CO2/CH4 separation: A review. *International Journal of Greenhouse Gas Control.* 2013;12:84-107.
17. Hussain A, Nasir H, Ahsan M. Process Design Analyses of CO2 Capture from Natural Gas by Polymer Membrane. *J.Chem.Soc.Pak.* 2014;36(3):11.
18. Scholes CA, Stevens GW, Kentish SE. Membrane gas separation applications in natural gas processing. *Fuel.* 2012;96:15-28.
19. G. D. Corporation G. - The Solver Manuals, GAMS Dev. Corp. 2013.

20. Gorissen H. Temperature changes involved in membrane gas separations. *Chemical Engineering and Processing: Process Intensification.* 1987/08/01 1987;22(2):63-67.
21. Ahmad F, Lau KK, Shariff AM, Fong Yeong Y. Temperature and pressure dependence of membrane permeance and its effect on process economics of hollow fiber gas separation system. *Journal of Membrane Science.* 2013;430:44-55.
22. Yee TF, Grossmann IE. Simultaneous optimization models for heat integration-II. Heat exchanger network synthesis. *Comput. Chem. Eng.* 1990;14(10):1165-1184.
23. Turton R, Bailie RC, Whiting WB, Shaeiwitz JA, Bhattacharyya D. *Analysis, synthesis, and design of chemical processes*2012.
24. U.S. Energy Information Administration, Average Price of Electricity to Ultimate Customers by End-Use Sector. 2015. Accessed: 06-Feb-2016. https://www.eia.gov/electricity/monthly/epm_table_grapher.cfm?t=epmt_5_6_a.
25. Binns M, Lee S, Yeo Y-K, et al. Strategies for the simulation of multi-component hollow fibre multi-stage membrane gas separation systems. *Journal of Membrane Science.* 2016;497:458-471.
26. Gilassi S, Rahmanian N. Mathematical modelling and numerical simulation of CO2/CH4 separation in a polymeric membrane. *Applied Mathematical Modelling.* 2015;39(21):6599-6611.
27. Bounaceur R, Berger E, Pfister M, Ramirez Santos AA, Favre E. Rigorous variable permeability modelling and process simulation for the design of polymeric membrane gas separation units: MEMSIC simulation tool. *Journal of Membrane Science.* 2017;523:77-91.
28. Yates S, Zaki R, Arzadon A, Liu C, Chiou J. Thin Film Gas Separation Membranes. 2010;US 2010/0269698 A1.
29. Drioli E, Barbieri G, Royal Society of Chemistry (Great Britain). Membrane engineering for the treatment of gases. Cambridge: Royal Society of Chemistry; 2011.
30. Wu Y, Carroll JJ, Li Q. *Gas injection for disposal and enhanced recovery*: Wiley; 2014.
31. Baker RW. Future Directions of Membrane Gas Separation Technology. *Ind. Eng. Chem. Res.* 2002/03/01 2002;41(6):1393-1411.
32. Green D, Perry R. *Perry's Chemical Engineers' Handbook, Eighth Edition*: McGraw-Hill Education; 2007.
33. Caballero JA, Grossmann IE, Keyvani M, Lenz ES. Design of Hybrid Distillation−Vapor Membrane Separation Systems. *Ind. Eng. Chem. Res.* 2009/10/21 2009;48(20):9151-9162.
34. Smith R. *Chemical Process Design and Integration. Chichester*: Wiley; 2016.

Appendices

Appendix A. Model for the unsymmetrical cascade p = 2, q = 1

The mathematical model of the membrane cascade *p* = 2, *q* = 1 superstructure (Figure 2) comprises the equations shown below. For the nomenclature see Figure A.1.

A.1. CONSTRAINTS

a) Mixers for the inlet of each stage

- Material balance across feed mixer of stage E7

$$\begin{aligned} &F^m = CP^m \qquad \forall \quad m = E7 \\ &F_j^m = CP_j^m \qquad \forall \quad m = E7,\, j \in COMP \end{aligned} \tag{A.1}$$

- Material balance across feed mixer of stage S1

$$\begin{aligned} &Feed + RR^{E1} + CP^{S1} = F^{S1} \\ &Feed_j + RR_j^{E1} + CP_j^{S1} = F_j^{S1} \qquad \forall\, j \in COMP \end{aligned} \tag{A.2}$$

- Material balance across feed mixer of stage S6 and S7

$$\begin{aligned} &F^m = RR^{m-1} \qquad \forall m \ge S6 \\ &F_j^m = RR_j^{m-1} \qquad \forall m \ge S6,\, j \in COMP \end{aligned} \tag{A.3}$$

- Material balance across the rest of the feed mixers

$$\begin{aligned} &F^m = RR^{m-1} + CP^m \qquad \forall \quad m \ne E7, S1, m \le S5 \\ &F_j^m = RR_j^{m-1} + CP_j^m \qquad \forall \quad m \ne E7, S1, m \le S5, \quad j \in COMP \end{aligned} \tag{A.4}$$

b) Membrane Module

The gas flow pattern in the membrane modules is assumed to be cross-flow and the equations are based on the model presented by Caballero et al.[33].

- Material balance on the shell side

$$\left.\begin{array}{ll} F^m = R^m + JA^m & \\ F_j^m = R_j^m + JA_j^m & \forall\, j \in COMP \end{array}\right\} \forall m \in MEM \qquad (A.5)$$

- Material balance on the tube side

$$\left.\begin{array}{ll} P^m = JA^m + S^m & \\ P_j^m = JA_j^m + S_j^m & \forall\, j \in COMP \end{array}\right\} \forall m \in MEM \qquad (A.6)$$

- Flow across membrane

$$JA_{CO_2}^m = \left(Perm\right)\left(Area_M\right)^m \left(p_{in} z_{CO_2}^m - p_{out}^m y_{CO_2}^m\right) \qquad \forall m \in MEM \qquad (A.7)$$

$$\alpha = \frac{y_{CO_2}^m / y_{CH_4}^m}{z_{CO_2}^m / z_{CH_4}^m} \qquad \forall m \in MEM \qquad (A.8)$$

where $\left(Perm\right)$ is the permeability of the considered membrane and α, its selectivity. Note that both are known parameters.

- Relation between individual and total flows

$$\left.\begin{aligned}
F^m &= \sum_{j \in COMP} F_j^m \\
JA^m &= \sum_{j \in COMP} JA_j^m \\
R^m &= \sum_{j \in COMP} R_j^m \\
RR^m &= \sum_{j \in COMP} RR_j^m \\
P^m &= \sum_{j \in COMP} P_j^m \\
S^m &= \sum_{j \in COMP} S_j^m \\
CP^m &= \sum_{j \in COMP} CP_j^m
\end{aligned}\right\} \quad \forall m \in MEM \tag{A.9}$$

- Definition of molar fractions

$$\left.\begin{aligned}
&z_j^m = \frac{F_j^m}{F^m} \qquad \forall\, j \in COMP \\
&\sum_{j \in COMP} z_j^m = 1
\end{aligned}\right\} \quad \forall m \in MEM \tag{A.10}$$

$$\left.\begin{aligned}
&y_j^m = \frac{P_j^m}{P^m} \qquad \forall\, j \in COMP \\
&\sum_{j \in COMP} y_j^m = 1
\end{aligned}\right\} \quad \forall m \in MEM \tag{A.11}$$

$$\left.\begin{aligned}
&x_j^m = \frac{R_j^m}{R^m} \qquad \forall\, j \in COMP \\
&\sum_{j \in COMP} x_j^m = 1
\end{aligned}\right\} \quad \forall m \in MEM \tag{A.12}$$

- Permeate outlet temperature

Membrane gas separations involve temperature changes that can be negligible for some mixtures. However, in other cases, these temperature decreases can be very important and they must be taken into account. According to literature[20], membrane separations can be considered to be isenthalpic processes. Based on this assumption, correlations for temperature changes of CO_2 and CH_4 steams have been obtained with Aspen HYSYS and MATLAB (these correlations can be seen in Appendix C). The permeate outlet temperature is calculated following the equation below as a weighted arithmetic mean assuming negligible difference between Cp values:

$$\left(T_{out,M}\right)^m = \sum_{j\in COMP}\left(z_j^m\left(T_{out,M}\right)_j\right) \qquad \forall\ m \in MEM \qquad \text{(A.13)}$$

- Pressure constraints

Each membrane stage has to have an inlet pressure that is higher than its outlet pressure.

$$p_{in} \geq p_{out}^m \qquad \forall\ m \in MEM \qquad \text{(A.14)}$$

In addition, if a membrane sends its permeate to the previous stage as sweep, its outlet pressure must be higher than the outlet pressure of the previous one.

$$p_{out}^{m-1} \leq p_{out}^m \qquad \forall\ m \in MEM, m \geq E6 \qquad \text{(A.15)}$$

- Area constraint

The following constraint is useful to avoid a flowsheet with large membrane areas and small membrane areas at the same time. It is possible to relax this constraint.

$$\frac{\left(Area_M\right)^{S1}}{F^{S1}} = \frac{\left(Area_M\right)^m}{F^m} \qquad \text{(A.16)}$$

c) Mixers for the final products (material balances)

The stream $Permeate_j$ is a mixture of the permeate streams of E7 and the lateral permeate extractions $\left((LE_P)_j^m\right)$.

$$Permeate_j = P_j^{E7} + \sum_{m=E6}^{S7} (LE_P)_j^m \qquad \forall\, j \in COMP \tag{A.17}$$

In the same way, the stream $Retentate_j$ is a mixture of the retentate stream of S7 and the lateral retentate extractions $\left((LE_R)_j^m\right)$.

$$Retentate_j = R_j^{S7} + \sum_{m=E7}^{S6} (LE_R)_j^m \qquad \forall\, j \in COMP \tag{A.18}$$

d) Permeate splitters

- Material balances and composition constraints

$$\left.\begin{aligned} & P_j^{m+1} = CP_j^{m-1} + S_j^m + (LE_P)_j^{m+1} \\ & \frac{P_j^{m+1}}{P^{m+1}} = \frac{CP_j^{m-1}}{CP^{m-1}} = \frac{S_j^m}{S^m} = \frac{(LE_P)_j^{m+1}}{(LE_P)^{m+1}} \end{aligned}\right\} \quad \forall\, m \in MEM,\, j \in COMP \tag{A.19}$$

- Definition of split ratios $\left((sr_{CP})^m \text{ and } (sr_{LE_P})^m\right)$

$$\left.\begin{aligned} & (sr_{CP})^m = \frac{CP_j^m}{P_j^{m+2}} \\ & 0 \le (sr_{CP})^m \le 1 \end{aligned}\right\} \quad \forall\, m \in MEM, m \le S5,\, j \in COMP \tag{A.20}$$

$$\left.\begin{aligned} & (sr_{LE_P})^m = \frac{(LE_P)_j^m}{P_j^m} \\ & 0 \le (sr_{LE_P})^m \le 1 \end{aligned}\right\} \quad \forall\, m \in MEM, m \ne E7,\, j \in COMP \tag{A.21}$$

- Relation between individual and total flow

$$\left(LE_P\right)^m = \sum_{j \in COMP} \left(LE_P\right)_j^m \qquad \forall\ m \in MEM, m \neq E7 \tag{A.22}$$

e) Retentate splitters

- Material balances and composition constraints

$$\left.\begin{aligned} & R_j^m = RR_j^m + \left(LE_R\right)_j^m \\ & \frac{R_j^m}{R^m} = \frac{RR_j^m}{RR^m} = \frac{\left(LE_R\right)_j^m}{\left(LE_R\right)^m} \end{aligned}\right\} \quad \forall\ m \in MEM, m \neq S7,\ j \in COMP \tag{A.23}$$

- Definition of split ratio $\left(\left(sr_{RR}\right)^m\right)$

$$\left.\begin{aligned} & \left(sr_{RR}\right)^m = \frac{RR_j^m}{R_j^m} \\ & 0 \leq \left(sr_{RR}\right)^m \leq 1 \end{aligned}\right\} \quad \forall\ m \in MEM, m \neq S7,\ j \in COMP \tag{A.24}$$

- Relation between individual and total flow

$$\left(LE_R\right)^m = \sum_{j \in COMP} \left(LE_R\right)_j^m \qquad \forall\ m \in MEM, m \neq S7 \tag{A.25}$$

f) Feed compressor

The work required for an adiabatic (isentropic) and staged compression[34] is given by:

$$W_{FC} = \frac{Feed}{\eta} \frac{\gamma}{\gamma - 1} R_p \left(T_{feed} + 273.15\right) N_{FC} \left(rp_{FC}^{\ \gamma-1/\gamma} - 1 \right) \tag{A.26}$$

where rp_{FC} is the compression ratio and is defined as:

$$rp_{FC} = \left(\frac{p_{in}}{p_{feed}} \right)^{1/N_{FC}} \tag{A.27}$$

The temperature rise for an isentropic compression can be determined from:

$$T_{out,FC} = \left(T_{feed} + 273.15\right)\left(1 + \frac{1}{\eta}\left(rp_{FC}^{\,\gamma-1/\gamma} - 1\right)\right) - 273.15 \tag{A.28}$$

It is worth noting that the compression ratio and the number of stages require lower and upper bounds:

$1 \le N_{FC} \le 4$
$1 \le rp_{FC} \le 4$

Between each compression stage, there are coolers that remove heat from the gas stream and, consequently, they reduce the amount of work necessary to compress the stream. The heat exchanged and the cooler area are is given by:

$$Q_{FC} = Feed \cdot C_{p,feed}\left(T_{out,FC} - T_{in}\right)N_{FC} \tag{A.29}$$

$$Q_{FC} = U\left(Area_{HE,FC}\right)\Delta T_{ML,FC} \tag{A.30}$$

where $\Delta T_{ML,FC}$ is the logarithmic mean temperature difference mean. In order to avoid numerical problems, Chen's approximation is used.

$$\begin{aligned} \Delta T_{ML,FC} &= \left(\theta_{1,FC}\theta_{2,FC}\frac{\left(\theta_{1,FC}+\theta_{2,FC}\right)}{2} \right)^{1/3} \\ \theta_{1,FC} &= T_{out,FC} - T_{out,CW} \\ \theta_{2,FC} &= T_{in} - T_{in,CW} \end{aligned} \tag{A.31}$$

In addition, a minimum approach temperature $\left(\Delta T_{min}\right)$ has to be satisfied to permit the energy exchange between the streams.

$$T_{in} - T_{in,CW} \geq \Delta T_{min}$$
$$T_{out,FC} - T_{out,CW} \geq \Delta T_{min} \tag{A.32}$$

g) Recycle compressors

The work required for each recycle compressor and its temperature rise are obtained following the procedure described earlier for the feed compressor:

$$W_C^m = \frac{CP^m}{\eta}\frac{\gamma}{\gamma-1}R_p\left(T_{out,M}{}^{m+2} + 273.15\right)N^m\left(\left(rp^m\right)^{\left(\gamma-1/\gamma\right)} - 1\right) \quad \forall\ m \in MEM, m \leq S5 \tag{A.33}$$

$$rp^m = \left(\frac{p_{in}}{p_{out}{}^{m+2}}\right)^{1/N^m} \qquad \forall\ m \in MEM, m \leq S5 \tag{A.34}$$

$$T_{out,C}{}^m = \left(T_{out,M}{}^{m+2} + 273.15\right)\left(1 + \frac{1}{\eta}\left(rp^{m\left(\gamma-1/\gamma\right)} - 1\right)\right) - 273.15 \quad \forall\ m \in MEM, m \leq S5 \tag{A.35}$$

The compression ratio and the number of stages of each compressor require lower and upper bounds as well.

$$\left.\begin{array}{l} 1 \leq N^m \leq 4 \\ 1 \leq rp^m \leq 4 \end{array}\right\} \qquad \forall\ m \in MEM, m \leq S5$$

The heat exchange and the cooler areas are given by:

$$Q_C{}^m = CP^m C_p{}^m\left(T_{out,C}{}^m - T_{in}\right)N^m \qquad \forall\ m \in MEM, m \leq S5 \tag{A.36}$$

$$Q_C{}^m = U\left(Area_{HE}{}^m\right)\Delta T_{ML}{}^m \qquad \forall\ m \in MEM, m \leq S5 \tag{A.37}$$

where:

$$\left.\begin{aligned}
&\Delta T_{ML}{}^{m} = \left(\theta_1{}^{m} \theta_2{}^{m} \frac{\left(\theta_1{}^{m} + \theta_2{}^{m}\right)}{2} \right)^{1/3} \\
&\theta_1{}^{m} = T_{out,C}{}^{m} - T_{out,CW} \\
&\theta_2{}^{m} = T_{in} - T_{in,CW}
\end{aligned}\right\} \quad \forall\ m \in MEM, m \le S5 \tag{A.38}$$

In this case, the minimum approach temperature $\left(\Delta T_{min}\right)$ has to be satisfied also.

$$T_{out,C}{}^{m} - T_{out,CW} \ge \Delta T_{min} \tag{A.39}$$

h) Turbine

The work done by a turbine can be calculated as follows:

$$W_T = \frac{\sum_{j \in COMP} Retentate_j}{\eta} \frac{\gamma}{\gamma - 1} R_p \left(T_{in} + 273.15\right) \left(1 - \left(\frac{p_{out,T}}{p_{in}} \right)^{\gamma-1/\gamma} \right) \tag{A.40}$$

Note that the lower and upper bounds of the turbine outlet pressure are:

$$1.01325 \le p_{out,T} \le p_{in}$$

i) Product specifications

- For product recovery:

$$Recovery(\%) = \frac{Retentate_{CH_4}}{Feed_{CH_4}} 100 \tag{A.41}$$

- For retentate purity:

$$x_{out,CO_2} = \frac{Retentate_{CO_2}}{\sum_{j \in COMP} Retentate_j} \tag{A.42}$$

- For permeate purity:

$$y_{out,CO_2} = \frac{Permeate_{CO_2}}{\sum_{j \in COMP} Permeate_j} \tag{A.43}$$

A.2. <u>DISJUNCTIONS</u>

The membrane superstructure shown in Figure 2 includes the following alternatives:

a) Turbine

The stream $Retentate_j$, which is at high-pressure, can be sent to a turbine, in order to use its energy and save electricity costs of recycle compressors. However, if turbine investment cost is higher than the savings, it must not be selected.

$$\begin{bmatrix} \boldsymbol{Y_T} \\ CT = f\left(W_T\right) \end{bmatrix} \veebar \begin{bmatrix} \neg \boldsymbol{Y_T} \\ p_{out,T} = p_{in} \\ CT = 0 \end{bmatrix} \tag{A.44}$$

This disjunction has been rewritten using Big M reformulation even though it is not explicitly stated in the text. The rest of the disjunctions are also reformulated in the same way.

b) Membrane

Despite the proposed superstructure containing fourteen different stages, the optimal solution is not going to include all of them. For this reason, it is essential that some of them be removable.

$$\left[\begin{array}{c} \boldsymbol{Y_M}^{\boldsymbol{m}} \\ \alpha = \dfrac{y_{CO_2}^m / y_{CH_4}^m}{z_{CO_2}^m / z_{CH_4}^m} \\ \dfrac{\left(Area_M\right)^{S1}}{F^{S1}} = \dfrac{\left(Area_M\right)^m}{F^m} \\ 1 \le \left(Area_M\right)^m \le 100 \\ 0 \le JA_j^m \le 50 \\ 0 \le \left(sr_{LE_P}\right)^m \le 1 \qquad \forall m \ge S1 \\ 0 \le \left(sr_{LE_P}\right)^{m+1} \le 1 \qquad \forall m \le E1 \\ 0 \le \left(sr_{RR}\right)^{m-1} \le 1 \qquad \forall m \ge S1 \\ 0 \le \left(sr_{RR}\right)^m \le 1 \qquad \forall m \le E1 \end{array}\right] \veebar \left[\begin{array}{c} \neg \boldsymbol{Y_M}^{\boldsymbol{m}} \\ p_{out}^m = p_{out}^{m+1} \\ \left(Area_M\right)^m = 0 \\ JA_j^m = 0 \\ \left(sr_{LE_P}\right)^m = 0 \qquad \forall m \ge S1 \\ \left(sr_{LE_P}\right)^{m+1} = 0 \qquad \forall m \le E1 \\ \left(sr_{RR}\right)^{m-1} = 1 \qquad \forall m \ge S1 \\ \left(sr_{RR}\right)^m = 1 \qquad \forall m \le E1 \end{array}\right] \tag{A.45}$$

c) Compressor

In order to obtain the optimal flowsheet, some compressors have to be removed and it can be achieved by this disjunction:

$$\left[\begin{array}{c} \boldsymbol{Y_C}^{\boldsymbol{m}} \\ 0 \le \left(sr_{CP}\right)^m \le 1 \\ CC = f\left(W_C^m\right) \\ CHE = f\left(Area_{HE}{}^m\right) \end{array}\right] \veebar \left[\begin{array}{c} \neg \boldsymbol{Y_C}^{\boldsymbol{m}} \\ \left(sr_{CP}\right)^m = 0 \\ CC = 0 \\ CHE = 0 \end{array}\right] \tag{A.46}$$

A.3. <u>LOGICAL RELATIONSHIPS</u>

a) If the compressor *m* exists, then the membrane *m* (which is fed by it) exists as well.

$$Y_C{}^m \Rightarrow Y_M{}^m \qquad \forall m \in MEM \tag{A.47}$$

b) If the compressor *m* exists, then the membrane *m+2* (which produces the permeate stream that is sent to this compressor) exists as well.

$$Y_C{}^m \Rightarrow Y_M{}^{m+2} \qquad \forall m \in MEM \tag{A.48}$$

c) If the membrane *m* does not exist, its compressor or the succeeding membrane compressor does not exist.

$$\neg Y_M{}^m \Rightarrow \neg Y_C{}^m \vee \neg Y_C{}^{m+1} \qquad \forall m \in MEM\,, m \le S5 \tag{A.49}$$

d) If compressor which feeds membrane *m* (C^m) and the compressor fed by membrane *m* do not exist (C^{m+2}), the membrane *m* does not exist. If this situation is not avoided, the stage would be connected in series with the others.

$$\neg Y_C{}^m \wedge \neg Y_C{}^{m-2} \Rightarrow \neg Y_M{}^m \qquad \forall m \in MEM\,, m \ne S1 \tag{A.50}$$

Now, these logical relationships are rewritten in terms of binary variables.

$$\begin{array}{ll}
\left.\begin{array}{l}
\left(1 - y_C{}^m\right) + y_M{}^m \ge 1 \\
\left(1 - y_C{}^m\right) + y_M{}^{m+2} \ge 1
\end{array}\right\} & \forall m \in MEM \\
\left(1 - y_C{}^m\right) + \left(1 - y_C{}^{m+1}\right) + y_M{}^m \ge 1 & \forall m \in MEM\,, m \le S5 \\
\left(1 - y_M{}^m\right) + y_C{}^m + y_C{}^{m-2} \ge 1 & \forall m \in MEM\,, m \ne S1
\end{array} \tag{A.51}$$

Note that the stage S1 always exists $\left(y_M{}^{S1} = 1\right)$.

Appendix B. Model for the unsymmetrical cascade *p* = 1, *q* = 2

In this Appendix, the mathematical model of the superstructure *p* = 1, *q* = 2 (Figure 3) is described. This model shares many equations with the previous one (Appendix A). For this reason this Appendix includes just the different equations. For nomenclature see Figure B.1.

B.1. CONSTRAINTS

a) Mixers for the inlet of each stage

- Material balance across feed mixer of stage E7: (A.1)
- Material balance across feed mixer of stage S1

$$\begin{aligned} &Feed + RR1^{E1} + RR2^{E2}\, CP^{S1} = F^{S1} \\ &Feed_j + RR1_j^{E1} + RR2_j^{E2}\, CP_j^{S1} = F_j^{S1} \qquad \forall\, j \in COMP \end{aligned} \tag{B.52}$$

- Material balance across feed mixer of stage S7

$$\begin{aligned} &F^m = RR1^{m-1} + RR2^{m-2} \\ &F_j^m = RR1_j^{m-1} + RR2_j^{m-2} \qquad \forall j \in COMP \end{aligned} \tag{B.53}$$

- Material balance across the rest of the feed mixers

$$\begin{aligned} &F^m = RR1^{m-1} + RR2^{m-2} + CP^m \qquad \forall \quad m \neq E7, S1, S7 \\ &F_j^m = RR1_j^{m-1} + RR2_j^{m-2} + CP_j^m \qquad \forall \quad m \neq E7, S1, S7, \quad j \in COMP \end{aligned} \tag{B.54}$$

b) Membrane Module: (A.5) - (A.16)

c) Mixers for the final products: (A.17) - (A.18)

d) Permeate splitters

- Material balances and composition constraints

$$\left.\begin{aligned} & P_j^{m+1} = CP_j^m + S_j^m + \left(LE_P\right)_j^{m+1} \\ & \frac{P_j^{m+1}}{P^{m+1}} = \frac{CP_j^m}{CP^m} = \frac{S_j^m}{S^m} = \frac{\left(LE_P\right)_j^{m+1}}{\left(LE_P\right)^{m+1}} \end{aligned}\right\} \quad \forall\ m \in MEM, m \le S6, j \in COMP \qquad \text{(B.55)}$$

- Definition of split ratios $\left(\left(sr_{CP}\right)^m \text{ and } \left(sr_{LE_P}\right)^m\right)$: (A.21)

$$\left.\begin{aligned} & \left(sr_{CP}\right)^m = \frac{CP_j^m}{P_j^{m+1}} \\ & 0 \le \left(sr_{CP}\right)^m \le 1 \end{aligned}\right\} \quad \forall\ m \in MEM, m \le S6, j \in COMP \qquad \text{(B.56)}$$

- Relation between individual and total flow: (A.22)

e) Retentate splitters

- Material balances and composition constraints

$$\left.\begin{aligned} & R_j^m = RR1_j^m + RR2_j^m + \left(LE_R\right)_j^m \\ & \frac{R_j^m}{R^m} = \frac{RR1_j^m}{RR1^m} = \frac{RR2_j^m}{RR2^m} = \frac{\left(LE_R\right)_j^m}{\left(LE_R\right)^m} \end{aligned}\right\} \quad \forall\ m \in MEM, j \in COMP \qquad \text{(B.57)}$$

- Definition of split ratio $\left(\left(sr_{RR1}\right)^m \text{ and } \left(sr_{RR2}\right)^m\right)$

$$\left.\begin{aligned} & \left(sr_{RR1}\right)^m = \frac{RR1_j^m}{R_j^m} \\ & 0 \le \left(sr_{RR1}\right)^m \le 1 \end{aligned}\right\} \quad \forall\ m \in MEM, m \ne S7, j \in COMP \qquad \text{(B.58)}$$

$$\left.\begin{aligned} & \left(sr_{RR2}\right)^m = \frac{RR2_j^m}{R_j^m} \\ & 0 \le \left(sr_{RR2}\right)^m \le 1 \end{aligned}\right\} \quad \forall\ m \in MEM, m \le S5, j \in COMP \qquad \text{(B.59)}$$

- Relation between individual and total flow: (A.25)

f) Feed compressor: (A.26) - (A.32)

g) Recycle compressors: (A.36) - (A.39)

The work required for each recycle compressor and its temperature rise are obtained following the procedure described earlier:

$$W_C^m = \frac{CP^m}{\eta}\frac{\gamma}{\gamma-1}R_p\left(T_{out,M}{}^{m+1}+273.15\right)N^m\left(\left(rp^m\right)^{\left(\gamma-1/\gamma\right)}-1\right) \quad \forall\ m\in MEM, m\le S6 \quad \text{(B.60)}$$

$$rp^m = \left(\frac{p_{in}}{p_{out}{}^{m+1}}\right)^{1/N^m} \qquad \forall\ m\in MEM, m\le S6 \quad \text{(B.61)}$$

$$T_{out,C}{}^m = \left(T_{out,M}{}^{m+1}+273.15\right)\left(1+\frac{1}{\eta}\left(rp^{m\left(\gamma-1/\gamma\right)}-1\right)\right)-273.15 \quad \forall\ m\in MEM, m\le S6 \quad \text{(B.62)}$$

h) Turbine: (A.40)

i) Product specifications: (A.41) - (A.43)

B.2. DISJUNCTIONS

a) Turbine: (A.44)

b) Membrane

As in Appendix A, it is necessary to remove some stages to obtain the optimal solution.

The change in membrane disjunction involves split ratios $\left(sr_{CP}\right)^m$ and $\left(sr_{LE_P}\right)^m$ only.

$$\begin{bmatrix} \boldsymbol{Y_M}^{\boldsymbol{m}} \\ \alpha = \dfrac{y^m_{CO_2} / y^m_{CH_4}}{z^m_{CO_2} / z^m_{CH_4}} \\ \dfrac{\left(Area_M\right)^{S1}}{F^{S1}} = \dfrac{\left(Area_M\right)^m}{F^m} \\ 1 \le \left(Area_M\right)^m \le 100 \\ 0 \le JA^m_j \le 50 \\ 0 \le \left(sr_{LE_P}\right)^m \le 1 \qquad \forall m \ge S1 \\ 0 \le \left(sr_{LE_P}\right)^{m+1} \le 1 \qquad \forall m \le E1 \\ 0 \le \left(sr_{RR1}\right)^{m-1} \le 1 \qquad \forall m \ge E7 \\ 0 \le \left(sr_{RR2}\right)^{m-1} \le 1 \qquad \forall m \ge E7 \end{bmatrix} \veebar \begin{bmatrix} \neg \boldsymbol{Y_M}^{\boldsymbol{m}} \\ p^m_{out} = p^{m+1}_{out} \\ \left(Area_M\right)^m = 0 \\ JA^m_j = 0 \\ \left(sr_{LE_P}\right)^m = 0 \qquad \forall m \ge S1 \\ \left(sr_{LE_P}\right)^{m+1} = 0 \qquad \forall m \le E1 \\ \left(sr_{RR1}\right)^{m-1} = 1 \qquad \forall m \ge E7 \\ \left(sr_{RR2}\right)^{m-1} = 0 \qquad \forall m \ge E7 \end{bmatrix} \tag{B.63}$$

c) **Compressor:** (A.46)

B.3. LOGICAL RELATIONSHIPS

a) If the compressor *m* exists, then the membrane *m* (which is fed by it) exists as well.

$$Y_C{}^m \Rightarrow Y_M{}^m \qquad \forall m \in MEM \tag{B.64}$$

b) If the compressor *m* exists, then the membrane *m+1* (which produces the permeate stream that is sent to this compressor) exists as well.

$$Y_C{}^m \Rightarrow Y_M{}^{m+1} \qquad \forall m \in MEM \tag{B.65}$$

c) The membranes have to be consecutive.

$$\begin{aligned} &Y_M{}^{m+1} \Rightarrow Y_M{}^m \qquad \forall m \in MEM, m \geq S1 \\ &Y_M{}^{m-1} \Rightarrow Y_M{}^m \qquad \forall m \in MEM, m \leq E1 \end{aligned} \tag{B.66}$$

d) If compressor which feeds membrane *m* (C^m) and the compressor fed by membrane *m* do not exist (C^{m+1}), the membrane *m* does not exist. If this situation is not avoided, the stage would be connected in series with the others.

$$\neg Y_C{}^m \wedge \neg Y_C{}^{m-1} \Rightarrow \neg Y_M{}^m \qquad \forall m \in MEM, m \neq E7, S1 \tag{B.67}$$

Now, these logical relationships are rewritten in terms of binary variables.

$$\begin{aligned} &\left.\begin{aligned} &\left(1-y_C{}^m\right)+y_M{}^m \geq 1 \\ &\left(1-y_C{}^m\right)+y_M{}^{m+1} \geq 1 \end{aligned}\right\} \qquad \forall m \in MEM \\ &\left(1-y_M{}^{m+1}\right)+y_M{}^m \geq 1 \qquad \forall m \in MEM, m \geq S1 \\ &\left(1-y_M{}^{m-1}\right)+y_M{}^m \geq 1 \qquad \forall m \in MEM, m \leq E1 \\ &\left(1-y_M{}^m\right)+y_C{}^m+y_C{}^{m-1} \geq 1 \qquad \forall m \in MEM, m \neq E7, S1 \end{aligned} \tag{B.68}$$

Note that the stage S1 always exists $\left(y_M{}^{S1}=1\right)$.

Appendix C. Correlations

In this appendix we present the correlations used.

C.1. Properties

a) Temperature changes

Temperature of a CO_2 stream (Aspen HYSYS):

$$\left(T_{out,M}\right)_{CO_2} = 2.643 + 0.9014\left(T_{in}\right) - 1.39\left(p_{in} - p_{out}{}^{m}\right) + 0.01587\left(T_{in}\left(p_{in} - p_{out}^{m}\right)\right) - 0.009248\left(p_{in} - p_{out}^{m}\right)^2 \quad \text{(C.1)}$$

Temperature of a CH_4 stream (Aspen HYSYS):

$$\left(T_{out,M}\right)_{CH_4} = -2.578 + 1.082\left(T_{in}\right) - 0.4447\left(p_{in} - p_{out}{}^{m}\right) \quad \text{(C.2)}$$

b) Heat capacity

Heat capacity fit (Aspen HYSYS):

$$C_p\left(\frac{kJ}{kmol\ K}\right) = 35.3 + 0.03088\left(T_{out,C}\left({}^{\circ}C\right)\right) + 2.435\left(y_{CO_2}\right) \quad \text{(C.3)}$$

C.2. Investment costs

a) Compressor cost (Centrifugal, axial and reciprocating)

Equation calculated for the compressor cost using the correlations presented by Turton et al[23]

($CEPCI_{2001}$ = 397, $CEPCI_{2015}$ = 550.4)

$$CC_{FC}\left(MM\$\right) = -1.044 \cdot 10^{-7}\left(W_{FC}\left(kW\right)\right)^2 + 1.126 \cdot 10^{-3}\left(W_{FC}\left(kW\right)\right) + 0.2076 \quad \text{(C.4)}$$

Equation calculated for the compressor cost, using the correlations presented by Smith[34]

($CEPCI_{2000}$ = 435.8, $CEPCI_{2015}$ = 550.4)

$$CC_C\left(MM\$\right) = -8.601\cdot10^{-8}\left(W_C\left(kW\right)\right)^2 + 2.475\cdot10^{-4}\left(W_C\left(kW\right)\right) + 0.06865 \qquad (C.5)$$

b) Cost heat exchanger (spiral plate)

Equation calculated for the heat exchanger cost, using the correlations presented by Turton et al[23] ($CEPCI_{2001}$ = 397, $CEPCI_{2015}$ = 550.4)

$$\begin{aligned} CHE_C\left(MM\$\right) &= 5.034\cdot10^{-6}\left(Area_{HE}\left(m^2\right)\right)^4 - 2.49\cdot10^{-4}\left(Area_{HE}\left(m^2\right)\right)^3 + \\ &+4.37\cdot10^{-3}\left(Area_{HE}\left(m^2\right)\right)^2 - 0.02876\left(Area_{HE}\left(m^2\right)\right) + 0.2546 \end{aligned} \qquad (C.6)$$

c) Cost turbine (Axial)

Equation calculated for the turbine cost, using the correlations presented by Turton et al[23] ($CEPCI_{2001}$ = 397, $CEPCI_{2015}$ = 550.4).

$$CT\left(MM\$\right) = 0.03235\ \left(W_T\left(MW\right)\right)^3 - 0.2818\ \left(W_T\left(MW\right)\right)^2 + 0.9364\ \left(W_T\left(MW\right)\right) + 0.5252 \qquad (C.7)$$

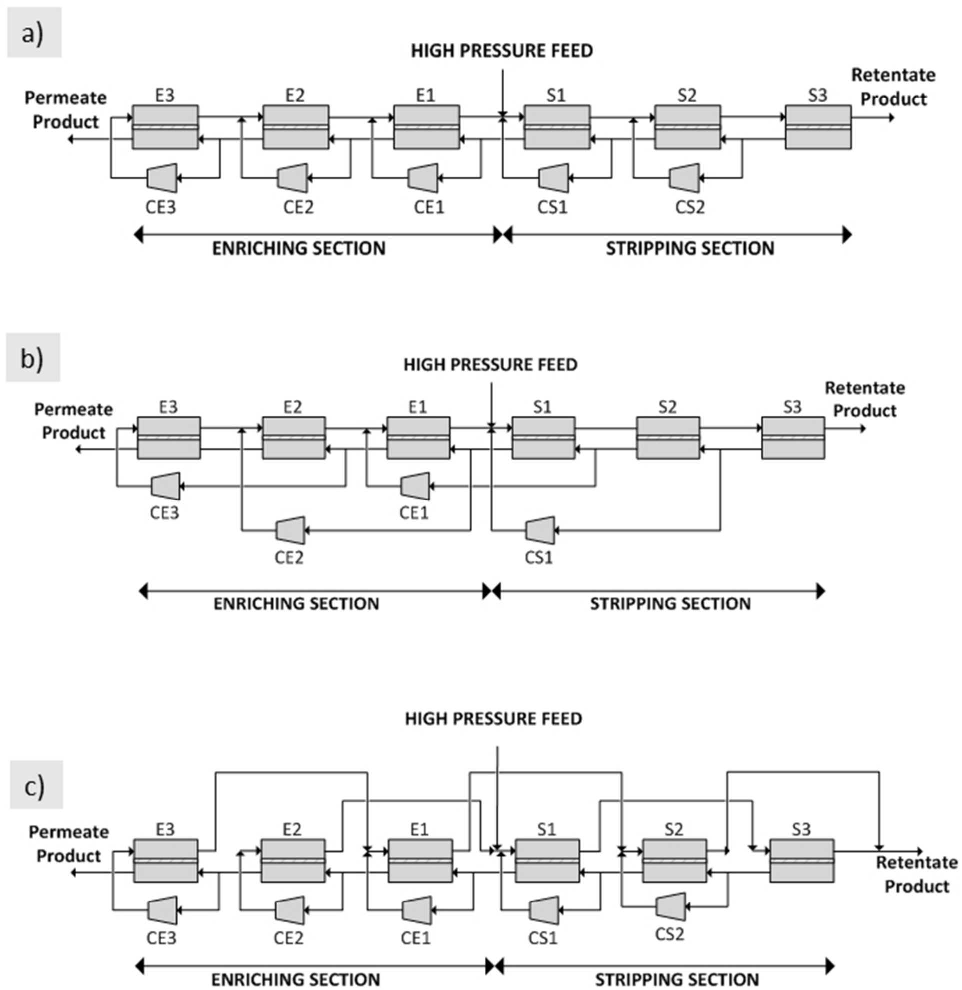

Figure 1. Membrane cascade schemes: a) symmetrical (p = 1, q = 1), b) unsymmetrical (p = 2, q = 1) and c) unsymmetrical cascade scheme (p = 1, q = 2).

189x190mm (96 x 96 DPI)

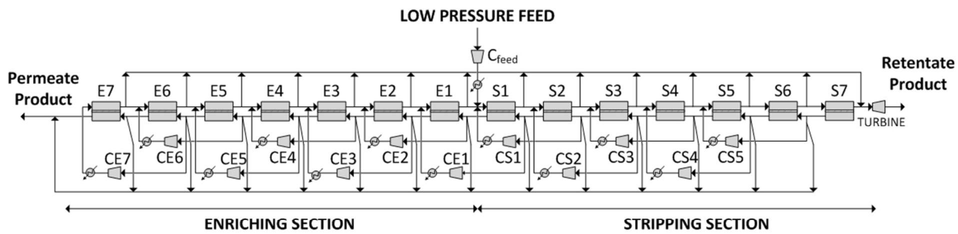

Figure 2. Unsymmetrical superstructure (p = 2, q = 1) with seven permeation stages in each section. This superstructure includes (p=1) in the calculation model (arrows not shown here)

338x190mm (96 x 96 DPI)

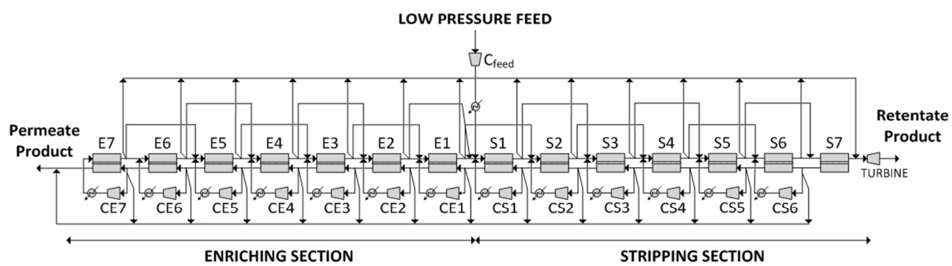

Figure 3. Unsymmetrical superstructure (p = 1, q = 2) with seven permeation stages in each section.

338x190mm (96 x 96 DPI)

$$
\begin{aligned}
\min_{x,Y_{ik}} \quad & z = GPC(x) \\
s.t. \quad & h(x) = 0 \\
& g(x) \leq 0 \\
& \bigvee_{i \in D_k} \begin{bmatrix} Y_{ik} \\ r_{ik}(x) \leq 0 \\ s_{ik}(x) = 0 \end{bmatrix} \qquad k \in K \\
& \Omega(Y) = True \\
& x^{lo} \leq x \leq x^{up} \\
& x \in \mathbb{R}^n,\ Y_{ik} \in \{True, False\},\ i \in D_k,\ k \in K
\end{aligned}
$$

Figure 4. Generalized Disjunctive Programming (GDP) model for the minimization of the Gas Processing Cost (GPC).

254x190mm (96 x 96 DPI)

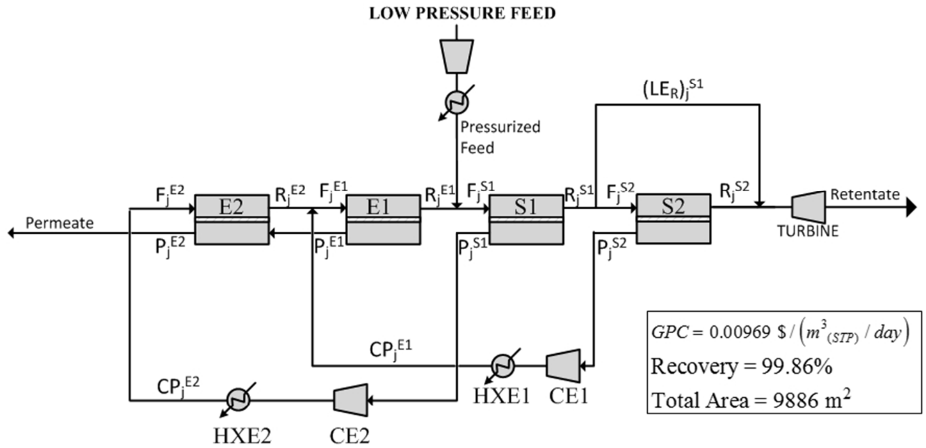

stream	F_j^{E2}	F_j^{E1}	F_j^{S1}	F_j^{S2}	R_j^{E2}	R_j^{E1}	R_j^{S1}	R_j^{S2}	P_j^{E2}	P_j^{E1}
CH_4 flow rate (kmol/min)	0.7803	1.2289	27.3385	18.4409	0.7803	1.1935	26.5582	17.9923	0.0354	0.0354
CO_2 flow rate (kmol/min)	2.2217	0.8191	3.1386	0.6367	0.4350	0.8191	0.9169	0.2526	2.3722	0.5855

stream	P_j^{S1}	P_j^{S2}	$(LE_R)_j^{S1}$	CP_j^{E2}	CP_j^{E1}	Pressurized feed	Retentate	Permeate
CH_4 flow rate (kmol/min)	0.7803	0.4486	8.1172	0.7803	0.4486	26.145	26.1096	0.0354
CO_2 flow rate (kmol/min)	2.2217	0.3841	0.2803	2.2217	0.3841	2.905	0.5328	2.3722

Figure 5. Optimized result for the membrane cascade along with its operating conditions, for crude gas natural sweetening. The names of the streams follow the nomenclature used in this paper. Feed molar fraction CH_4 = 0.9. Pressure of retentate streams = 65.5x10^5 Pa. Temperature of retentate streams = 74.6ºC. Pressure of the permeate stream = 1.01325x10^5 Pa. Membrane areas: E2 (545.3 m^2), E1 (339.1 m^2), S1 (5535.8 m^2), S2 (3465.2 m^2). Energy consumed by compressors: feed = 2221.2 kW; CE2 = 855.9 kW; CE1 = 250 kW. Turbine-recovered energy: 3327.1 kW. Turbine outlet pressure: 5.64x10^5 Pa.

254x190mm (96 x 96 DPI)

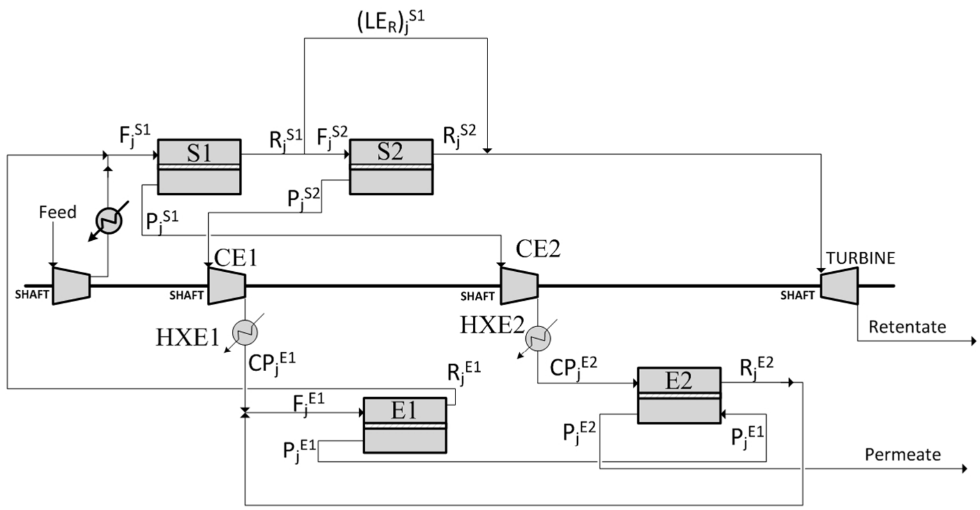

Figure 6. Optimized solution shown in Figure 5, now with the membrane modules redistributed in a way that emphasizes the common shaft (thick line), which the compressors and turbine share in order to recover part of the spent energy.

338x190mm (96 x 96 DPI)

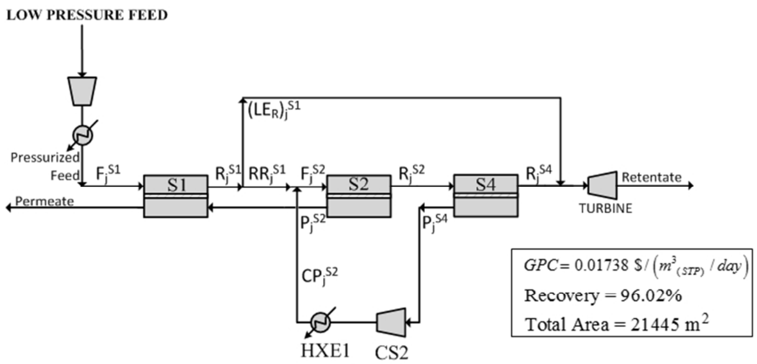

stream	F_j^{S1}	F_j^{S2}	F_j^{S4}	R_j^{S1}	R_j^{S2}	R_j^{S4}	RR_j^{S1}	P_j^{S2}
CH_4 flow rate (kmol/min)	11.620	11.067	10.852	11.373	10.852	10.633	10.848	0.215
CO_2 flow rate (kmol/min)	17.430	0.773	0.400	0.600	0.400	0.200	0.573	0.373

stream	P_j^{S4}	$(LE_R)_j^{S1}$	CP_j^{S2}	Retentate	Permeate
CH_4 flow rate (kmol/min)	0.219	0.525	0.219	11.158	0.462
CO_2 flow rate (kmol/min)	0.200	0.028	0.200	0.228	17.202

Figure 7. Optimized result for the membrane cascade along with its operating conditions, for enhanced oil recovery. The names of the streams follow the nomenclature used in this paper. Feed molar fraction CH_4 = 0.4. Pressure of retentate streams = 32.1x10^5 Pa. Temperature of retentate streams = 53.1ºC. Pressure of the permeate stream = 1.013x10^5 Pa. Membrane areas: S1 (13332 m^2), S2 (3712 m^2), S4 (4401 m^2). Energy consumed by compressors: feed = 867.3 kW; CS2 = 100.8 kW. Turbine-recovered energy: 968 kW. Turbine outlet pressure: 6.42x10^5 Pa.

254x190mm (96 x 96 DPI)

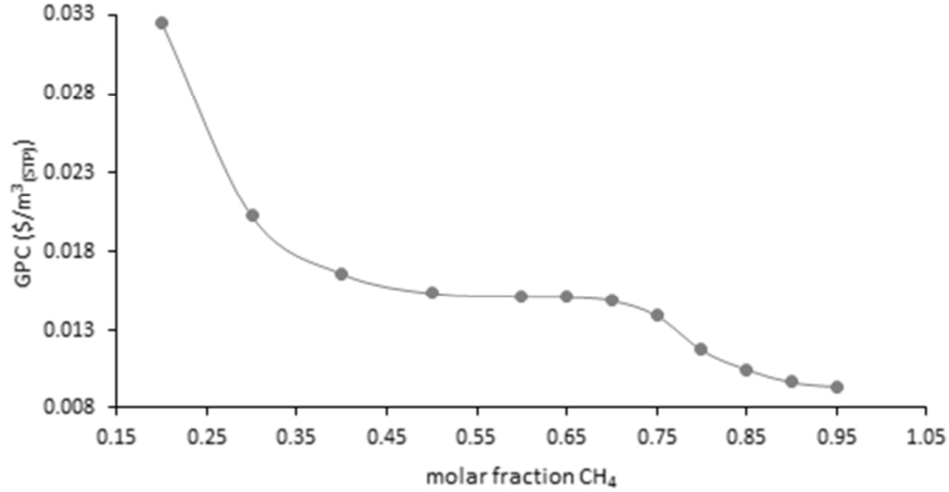

Figure 8. Sensitivity of the GPC to different values of the feed composition (same molar flow rate in the feed stream) for the crude gas sweetening case study.

139x70mm (96 x 96 DPI)

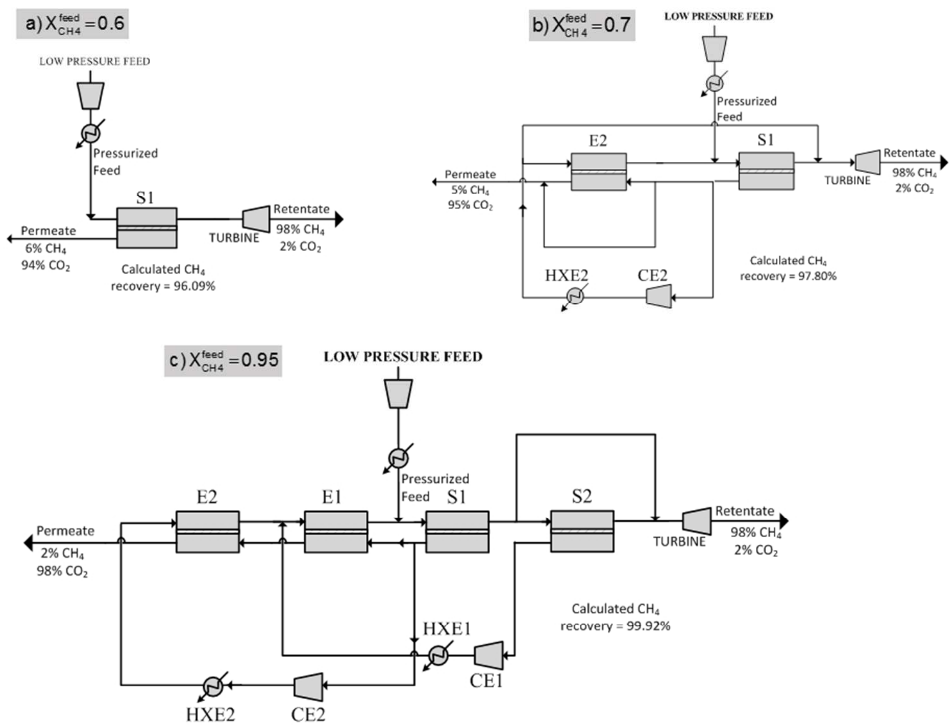

Figure 9. Different optimized layouts derived from the superstructure shown in Figure 2, for various feed compositions in the crude gas sweetening case study. This figure augments the information given in Fig 8. Note that, for the calculation, all compressors and the turbine in each figure in reality lie along the same shaft.

254x190mm (96 x 96 DPI)

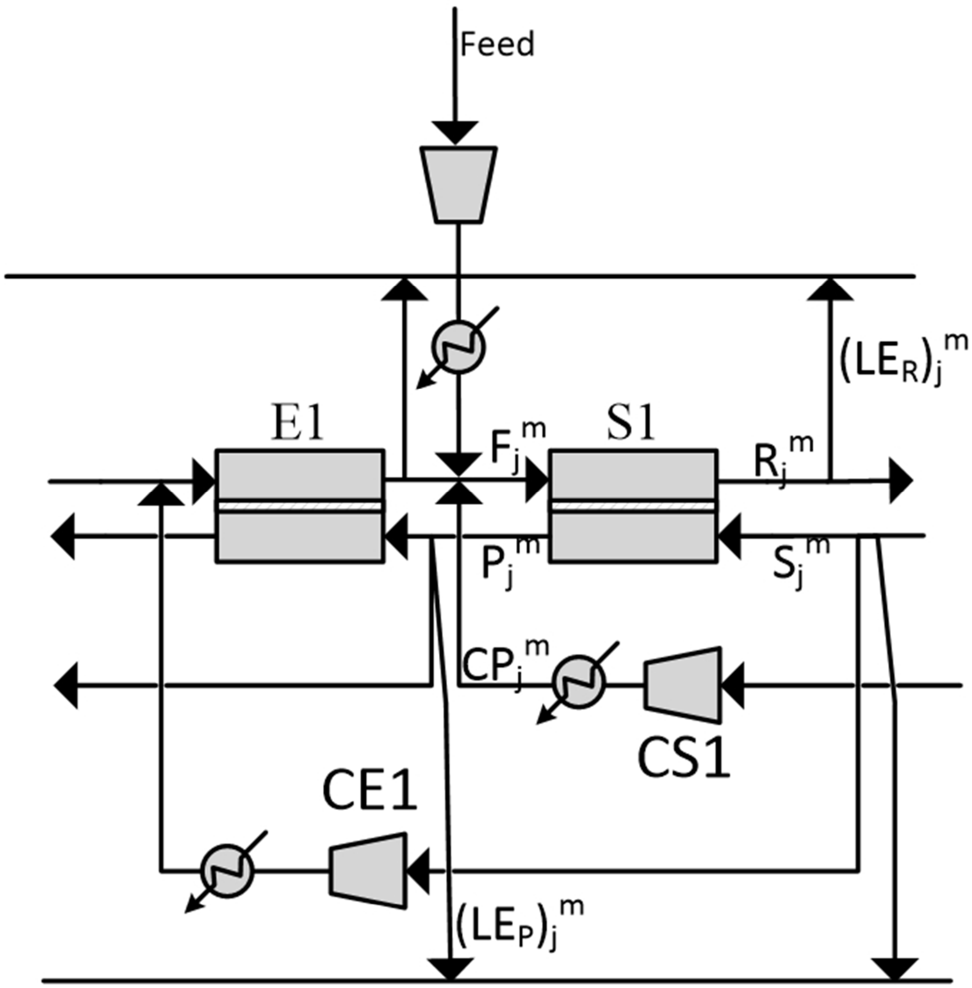

Figure A.1. Representation of the variables in the cascade p = 2, q = 1.
Figure A.1
184x190mm (96 x 96 DPI)

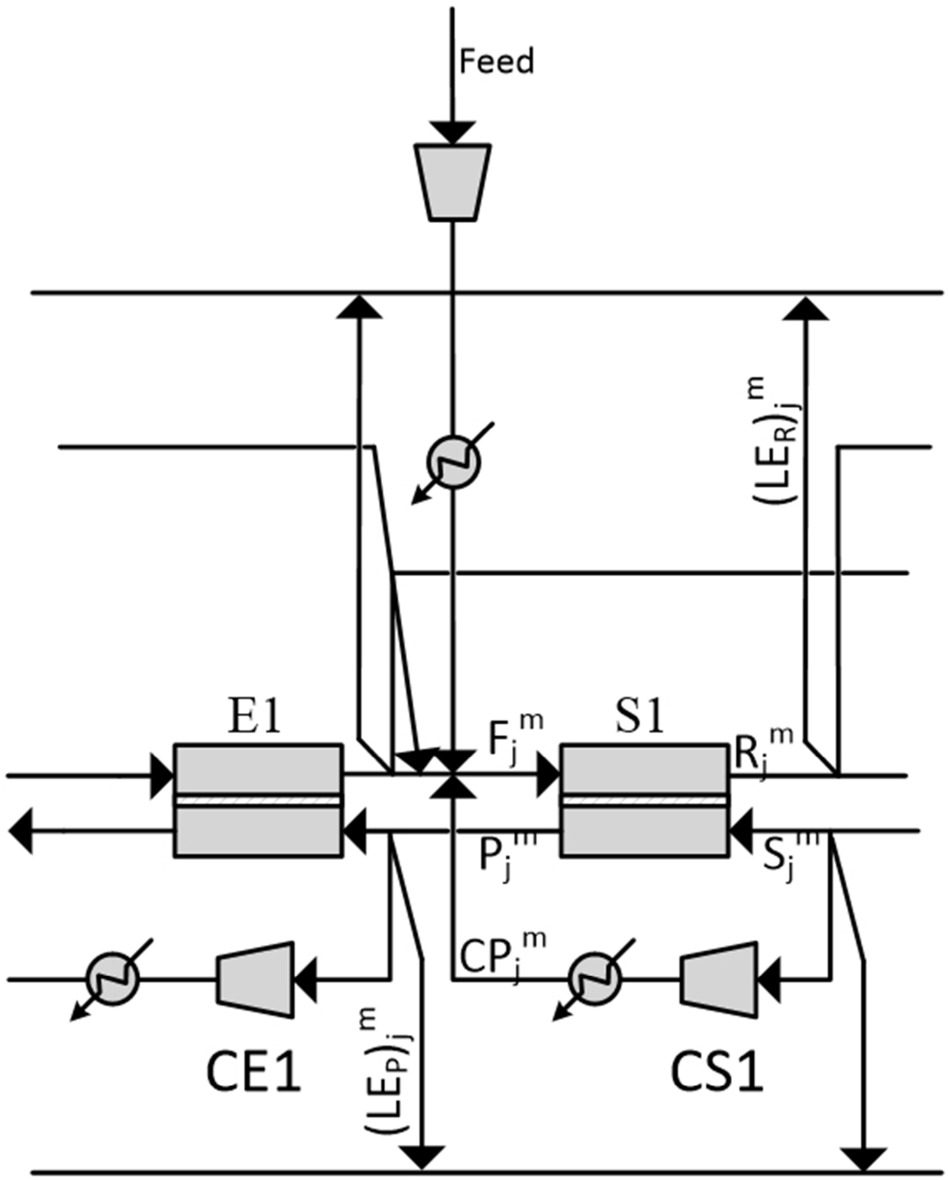

Figure B.1. Representation of the variables in the cascade *p* = 1, *q* = 2.
Figure B.1
150x190mm (96 x 96 DPI)

Table 1. Parameters and assumptions for the economic evaluation of the gas processing cost (GPC)[14].

Total plant investment (TPI)	$\boldsymbol{TPI = TFI + SC}$ **(1)**
Total membrane module cost (MC). Area values must be in m^2.	$MC = 50\frac{\$}{m^2}\sum_{m\,\in \text{membranes}} Area_m$
Installed compressor cost (CC)[a]	$CC = \sum_{m \in membranes} CC_{C_m} + CC_{FC}$ $CC_{C_m} = f\left(W_{C_m}\right)$; $CC_{FC} = f\left(W_{FC}\right)$
Installed heat exchanger cost (CHE)[a]	$CHE = \sum_{m\,\in \text{membranes}} CHE_{C_m} + CHE_{FC}$ $CHE_{C_m} = f\left(Area_{HE_m}\right); CHE_{FC} = f\left(Area_{HE,FC}\right)$
Installed turbine cost (CT)[a]	$CT = f\left(W_T\right)$
Fixed cost (FC)	$FC = MC + CC + CT + CHE$
Base plant cost (BPC)	$BPC = 1.12\ FC$
Project contingency (PC)	$PC = 0.2\ BPC$
Total facilities investment (TFI)	$TFI = BPC + PC$
Start-up cost (SC)	$SC = 0.1\ VOM$
Annual variable operating and maintenance cost (VOM)	$\boldsymbol{VOM = CMC + LTI + DL + LOC + MRC + UC}$ **(10)**
Contract and material maintenance cost (CMC)	$CMC = 0.05\ TFI$
Local taxes and insurance (LTI)	$LTI = 0.015\ TFI$
Direct labor cost (DL)[b]	$DL = No.workers\left(15\frac{\$}{h}\ 8\frac{h}{d}\ 365\frac{d}{y}\ OSF\right)$
Labor overhead cost (LOC)	$LOC = 1.15\ DL$
Membrane replacement cost (MRC)	$MRC = 25\frac{\$}{m^2}\frac{\sum_{m\,\in \text{membranes}} Area_m}{ML}$
Utility cost (UC)	$UC = C_{Electricity} + C_{Cooling}$
Electricity cost ($C_{Electricity}$)	$C_{Electricity} = EP\left(W_{FC} + \sum_{m\,=\,E7}^{S6} W_{C_m} - W_T\right)\left(\frac{24\ h}{1\ d}\ \frac{365\ d}{1\ y}\ OSF\right)$
Cooling cost ($C_{Cooling}$)	$C_{Cooling} = RP\left(Q_{FC} + \sum_{m\,\in \text{membranes}} Q_{C_m}\right)\left(\frac{3600\ s}{1\ h}\ \frac{24\ h}{1\ d}\ \frac{365\ d}{1\ y}\ OSF\right)$
Annual cost of CH_4 lost in permeate (CH_4LS)	$\boldsymbol{CH_4LS = NGLS \cdot NHV \cdot NWP}$
Annual natural gas lost (NGLS)	$NGLS = 365 \cdot OSF \cdot Q_V^{Feed}\ \frac{Permeate_{CH_4}}{\sum_{j \in COMP} Permeate_j}\ z_{CH_4}^{Feed}$

Gas processing cost (GPC)[c,d]	$GPC = \dfrac{CRC + CH_4LS + VOM}{365 \cdot OSF \cdot Q_V^{Feed}\left(1 - SCE\right)\dfrac{1000\ A}{B}}$
Annual capital related cost (CRC)	$CRC = 0.2\ TPI$
Stage-cut equivalent	$SCE = \dfrac{\sum_{j \in COMP} Permeate_j}{Feed} 100$
Other assumptions	
Number of workers (No. workers)[e]	4.5 workers
Electricity price (EP)[f]	\$ 0.02 /MJ
Refrigeration price (RW)[e]	\$ $4.43 \cdot 10^{-6}$ /kJ
Membrane life (*ML*)	4 years
Wellhead price of crude natural gas (NWP)	1.9 \$/GJ
Heating value of natural gas (NHV)	41.94 kJ/$m^3_{(STP)}$
On-stream factor (OSF)	0.96

[a] Correlations for CC_{C_m}, CC_{FC}, CHE_{C_m}, CHE_{FC} and CT can be found in Appendix C.

[b] DL is based on 8 h per day.

[c] A = 26.84 standard m^3/day (101.325 kPa at 0ºC)

[d] B = 1000 A.

[e] From[23]

[f] From[24]

Table 2. Membrane properties[28]

Material	Polymeric blend
Selectivity, α_{CO_2/CH_4}	24.8
Thickness (m)	0.5×10^{-6}
Permeance, P_{CO_2} ((m^3(STP)·m)/(m^2·s·Pa))	1.39×10^{-16}

Table 3. Data collected for crude natural gas sweetening & enhanced oil recovery.

	Natural Gas Sweetening	Enhanced Oil Recovery
Feed conditions		
Pressure (Pa), p_{feed}	20×10^5 [a]	
Temperature (ºC), T_{feed}	40 [a]	
Mole flow (kmol h^{-1}), $Feed$	1743 (or 939452.77 $m^3_{(STP)}$ [b])	
Mole fraction, z_j^{Feed}		
- CH_4	0.9 [b]	0.4 [b]
- CO_2	0.1	0.6
Outlet conditions		
Permeate pressure (Pa), p_{out}^{E7}	1.01325×10^5	
Product requirements		
Recovery CH_4	>95%	
Permeate mole fraction, y_{out,CO_2}	–	>0.95 [c]
Retentate mole fraction, x_{out,CO_2}	$\leq$ 0.02 [d]	
Membrane assumptions		
Thickness (m)	0.5×10^{-6} [d]	
Permeability (kmol m^{-2} s^{-1} Pa^{-1})	$1.15 \cdot 10^{-10}$ [e]	
Other data		
Isentropic efficiency, η	0.7	
Feed heat capacity, $C_{p,feed}$	41.66	

Ratio C_p/C_v, γ	1.351
Overall heat exchanger coefficient ($W\ m^{-2}\ K^{-1}$), U	580 [f]
Inlet temperature of cooling water (ºC) $T_{in,CW}$	5
Outlet temperature of cooling water (ºC) $T_{out,CW}$	15
Minimum approach temperature (ºC), ΔT_{min}	10

[a] From[29]

[b] From[2]

[c] From[30]

[d] From[31]

[e] $\text{Permeability} = \frac{\text{Permeance}}{\text{Thickness}}$

[f] From[32]

Table 4. Summary of model statistics and CPU time.

	Natural Gas Sweetening	Enhance Oil Recovery
Equations	1230	1230
Continuous variables	703	703
Discrete variables	39	39
CPU time (s): Intel® Core™ i5-3230M 2.60GHz	108.469	19.172